Received: 26 July 2022 | Accepted: 25 November 2022

DOI: 10.1111/gcb.16543

Global Change Biology WILEY

RESEARCH ARTICLE

A critical thermal transition driving spring phenology of Northern Hemisphere conifers

Jian-Guo Huang[1] | Yaling Zhang[2,3] | Minhuang Wang[4] | Xiaohan Yu[5] | Annie Deslauriers[6] | Patrick Fonti[7] | Eryuan Liang[8] | Harri Mäkinen[9] | Walter Oberhuber[10] | Cyrille B. K. Rathgeber[11] | Roberto Tognetti[12] | Václav Treml[13] | Bao Yang[14] | Lihong Zhai[2,3] | Jiao-Lin Zhang[15] | Serena Antonucci[12] | Yves Bergeron[16] | Jesus Julio Camarero[17] | Filipe Campelo[18] | Katarina Čufar[19] | Henri E. Cuny[20] | Martin De Luis[21] | Marek Fajstavr[22] | Alessio Giovannelli[23] | Jožica Gričar[24] | Andreas Gruber[10] | Vladimír Gryc[22] | Aylin Güney[25,26] | Tuula Jyske[9] | Jakub Kašpar[13,27] | Gregory King[7,28] | Cornelia Krause[6] | Audrey Lemay[6] | Feng Liu[29] | Fabio Lombardi[30] | Edurne Martinez del Castillo[21] | Hubert Morin[6] | Cristina Nabais[18] | Pekka Nöjd[9] | Richard L. Peters[7,31] | Peter Prislan[19] | Antonio Saracino[32] | Vladimir V. Shishov[33] | Irene Swidrak[10] | Hanuš Vavrčík[22] | Joana Vieira[18] | Qiao Zeng[34] | Yu Liu[35] | Sergio Rossi[6]

[1]MOE Key Laboratory of Biosystems Homeostasis and Protection, College of Life Sciences, Zhejiang University, Hangzhou, China

[2]Key Laboratory of Vegetation Restoration and Management of Degraded Ecosystems, Guangdong Provincial Key Laboratory of Applied Botany, South China Botanical Garden, Chinese Academy of Sciences, Guangzhou, China

[3]South China National Botanical Garden, Guangzhou, China

[4]Department of Ecology, School of Life Sciences, State Key Laboratory of Biocontrol, Sun Yat-sen University, Guangzhou, China

[5]School of Engineering and Built Environment, Griffith University, Brisbane, Australia

[6]Laboratoire sur les écosystèmes terrestres boréaux, Département des Sciences Fondamentales, Université du Québec à Chicoutimi, Chicoutimi, Quebec, Canada

[7]Swiss Federal Research Institute for Forest, Snow and Landscape Research WSL, Birmensdorf, Switzerland

[8]State Key Laboratory of Tibetan Plateau Earth System, Environment and Resources (TPESER), Institute of Tibetan Plateau Research, Chinese Academy of Sciences, Beijing, China

[9]Department of Forests, Natural Resources Institute Finland, Espoo, Finland

[10]Department of Botany, Leopold-Franzens-University of Innsbruck, Innsbruck, Austria

[11]Université de Lorraine, AgroParisTech, INRAE Silva, Nancy, France

[12]Dipartimento di Agricoltura, Ambiente e Alimenti, Università degli Studi del Molise, Campobasso, Italy

[13]Department of Physical Geography and Geoecology, Charles University, Prague, Czech Republic

[14]Cold and Arid Regions Environmental and Engineering Research Institute, Chinese Academy of Sciences, Beijing, China

[15]CAS Key Laboratory of Tropical Forest Ecology, Xishuangbanna Tropical Botanical Garden, Chinese Academy of Sciences, Mengla, Yunnan, China

[16]Forest Research Institute, Université du Quebec en Abitibi-Témiscamingue, Rouyn-Noranda, Quebec, Canada

[17]Instituto Pirenaico de Ecología (IPE-CSIC), Zaragoza, Spain

[18]Centre for Functional Ecology, Department of Life Sciences, University of Coimbra, Coimbra, Portugal

[19]Biotechnical Faculty, University of Ljubljana, Ljubljana, Slovenia

[20]IGN, Direction Interrégionale NordEst, Champigneulles, France

[21]Department of Geography and Regional Planning, Environmental Science Institute, University of Zaragoza, Zaragoza, Spain

[22]Department of Wood Science and Wood Technology, Mendel University in Brno, Brno, Czech Republic

Jian-Guo Huang and Yaling Zhang contributed equally to this work.

[23]CNR – Istituto di Ricerca sugli Ecosistemi Terrestri, IRET, Sesto Fiorentino, Italy
[24]Slovenian Forestry Institute, Ljubljana, Slovenia
[25]Institute of Botany, University of Hohenheim, Stuttgart, Germany
[26]Izmir Katip Çelebi University, Faculty of Forestry, Izmir, Turkey
[27]Department of Forest Ecology, Silva Tarouca Research Institute for Landscape and Ornamental Gardening, Průhonice, Czech Republic
[28]Department of Sciences, University of Alberta, Camrose, Alberta, Canada
[29]Key Laboratory of Aquatic Botany and Watershed Ecology, Wuhan Botanical Garden, Chinese Academy of Sciences, Wuhan, China
[30]AGRARIA Department, Mediterranean University of Reggio Calabria, Reggio Calabria, Italy
[31]Laboratory of Plant Ecology, Department of Plants and Crops, Faculty of Bioscience Engineering, Ghent University, Ghent, Belgium
[32]Department of Agricultural Sciences, University of Naples Federico II, Portici-Napoli, Italy
[33]Institute of Economics and Trade, Siberian Federal University, Krasnoyarsk, Russia
[34]Key Lab of Guangdong for Utilization of Remote Sensing and Geographical Information System, Guangdong Open Laboratory of Geospatial Information Technology and Application, Guangzhou Institute of Geography, Guangzhou, China
[35]The State Key Laboratory of Loess and Quaternary Geology, Institute of Earth Environment, Chinese Academy of Sciences, Xi'an, China

Correspondence
Yu Liu, The State Key Laboratory of Loess and Quaternary Geology, Institute of Earth Environment, Chinese Academy of Sciences, Xi'an, China.
Email: liuyu@loess.llqg.ac.cn

Funding information
National Natural Science Foundation of China, Grant/Award Number: 32001118, 32001138 and 32271653; Xinjiang Regional Collaborative Innovation Project, Grant/Award Number: 2022E01045; Zhejiang University, Grant/Award Number: 108000*1942222R1

Abstract

Despite growing interest in predicting plant phenological shifts, advanced spring phenology by global climate change remains debated. Evidence documenting either small or large advancement of spring phenology to rising temperature over the spatio-temporal scales implies a potential existence of a thermal threshold in the responses of forests to global warming. We collected a unique data set of xylem cell-wall-thickening onset dates in 20 coniferous species covering a broad mean annual temperature (MAT) gradient (−3.05 to 22.9°C) across the Northern Hemisphere (latitudes 23°–66° N). Along the MAT gradient, we identified a threshold temperature (using segmented regression) of 4.9 ± 1.1°C, above which the response of xylem phenology to rising temperatures significantly decline. This threshold separates the Northern Hemisphere conifers into cold and warm thermal niches, with MAT and spring forcing being the primary drivers for the onset dates (estimated by linear and Bayesian mixed-effect models), respectively. The identified thermal threshold should be integrated into the Earth-System-Models for a better understanding of spring phenology in response to global warming and an improved prediction of global climate-carbon feedbacks.

KEYWORDS
cell wall thickening, Northern Hemisphere conifer, photoperiod, spring forcing, winter chilling, xylem phenology

1 | INTRODUCTION

As an integrated response to environmental changes, forest spring phenology is interconnected with ecosystem functions and services, including forest productivity (Cuny et al., 2015), species distribution (Kharouba et al., 2018), and community assemblage (Piao et al., 2019). The advances in spring phenology are well appreciated as a major imprint of climate change impacts across all biomes (Menzel et al., 2006; Richardson et al., 2013), but are mostly focused on the onset of primary growth (Delpierre et al., 2016). Secondary growth, or xylem phenology, is also a key component of forest spring phenology but remains understudied until the development of the micro-sampling approach (Deslauriers et al., 2003; Huang et al., 2020).

Temperature has been widely recognized as a key driver for cambial reactivation of Northern Hemisphere conifers (Huang et al., 2020; Rossi et al., 2016). Warmer temperatures promote hormone production and the conversion of starch to sugar, thus breaking the dormancy (i.e., ecodormancy) and inducing cell division in the vascular cambium (Begum et al., 2018). These processes have been confirmed from experiments of localized heating of the stem (Oribe et al., 2003) and field observations of wood formation (Moser et al., 2010; Rossi et al., 2016).

More recently, studies on the onset of primary growth have demonstrated the declining effects of global warming on spring phenology, indicating a slowdown in the advancement of spring phenology, especially in warm ecosystems (Fu et al., 2015; Vitasse et al., 2018). For instance, larger advancements in spring phenology have been observed at higher altitudes, colder sites, and rural areas (Meng et al., 2020; Prevéy et al., 2017; Vitasse et al., 2018). Such differences in the advancing rates raise questions about the occurrence of critical thresholds along thermal gradients above which the process of advancement decreases significantly. However, despite the ecological importance of a potential transition temperature in shaping terrestrial biomes with climate warming, it has not been accurately incorporated into the Earth-System-Models (Delpierre et al., 2019; Huang et al., 2020), which jeopardizes the model performance in predicting phenological responses under future climate scenarios.

Trees require a sufficient forcing temperature above a threshold of 0–5°C for the resumption of xylem growth (Antonucci et al., 2015). On one hand, warming can accelerate the advancing rate through the accumulation of forcing temperature. On the other hand, warming imposes a higher forcing temperature requirement through the lower accumulation of chilling (i.e., the sum of low-temperature incidents informing that winter has passed) (Asse et al., 2018; Delpierre et al., 2019). Such a dual effect of warming could play a role in slowing down the advancement of spring phenology under warming conditions (Delpierre et al., 2019; Meng et al., 2020; Montgomery et al., 2020). Growth reactivation is also controlled by photoperiod over the Northern Hemisphere (Huang et al., 2020; Rossi et al., 2016). Photoperiod could constrain the advancement under warming conditions as spring phenological events tend to occur at a shorter photoperiod (Fu et al., 2019; Meng et al., 2020). Despite numerous hypotheses raised in the literature, the factors involved in the declining trend of tree spring phenology advancement remain to be disentangled.

Herein, we aimed to identify the threshold temperature at which the advancement of spring phenology to rising temperature drops significantly, and to elucidate the possible causes of the decline. We used "space-for-time approach," which is widely used in ecology for inference about future climate change impacts (Elmendorf et al., 2015; Peters et al., 2019), to tackle this problem. Recent studies have shown no virtual spatial bias for predicting the timing of cambial resumption (Delpierre et al., 2019; Huang et al., 2020). They suggest that species and site were not the main factors affecting the onset of wood formation of conifers across the Northern Hemisphere (Huang et al., 2020), which is far less affected by local adaptation than by environmental plasticity (Delpierre et al., 2019). Thus, with a scarcity of high-quality time series in xylem phenology, applying a space-for-time approach could be a reasonable alternative to project the impacts of climate change on wood phenology (Rossi et al., 2016). We, therefore, proposed that the spatial pattern of the onset dates of xylem phenological activities along the gradient of mean annual temperature (MAT) revealed in our study can provide a framework to examine the responses of secondary growth of forests to rising temperatures.

In this study, we compiled a large and unique data set of weekly cell-wall-thickening phenological measurements of 20 coniferous species from 75 sites over the Northern Hemisphere as surrogates for spring phenological activity. These sites spanned across a broad MAT gradient (−3.05°C to 22.9°C), from 23°11′ N to 66°12′ N, including boreal, temperate, Mediterranean, and subtropical biomes (Figure 3a and Table S1). The cell-wall-thickening process is part of the secondary growth of trees representing the progression from cell enlargement to cell wall thickening, lignification, and programmed cell death that generates the mature xylem (Figure S2) (Begum et al., 2013). This process ultimately accounts for 90% of the woody biomass production of forest trees (Cuny et al., 2015). Thus, weekly cell-wall-thickening phenological measurements offer a unique opportunity to describe the dynamics of the global carbon cycle and improve our ability to simulate the future of the Earth's system at a high temporal resolution.

2 | MATERIALS AND METHODS

2.1 | Field experiments and sample collection

Xylogenesis was monitored throughout the growing season from January–April to October–December according to the local climate of the sites. The monitoring years varied among the sampling sites from 1998 to 2016 (Table S1). At each site, from 1 to 55 adult dominant trees with upright, healthy trunks were selected for sampling. Wood microcores (2.5 mm in diameter × 25 mm long) were collected weekly (90%) or, on occasion, biweekly, from around the stems at breast height (1.3 ± 0.3 m) using a Trephor microcorer (Rossi et al., 2006). The samples usually contained several (or at least one) previous tree rings, as well as the developing annual layer with the cambial zone and adjacent phloem tissues. The microcores were stored immediately at 5°C in solutions of propionic or acetic acid mixed with formaldehyde or ethanol to avoid tissue deterioration and were then transported to the lab for further treatment. The microcores were dehydrated in ethanol and *D*-limonene and then embedded in paraffin or glycol methacrylate. Transverse sections 10–30 μm thick were cut from the samples with rotary or sledge microtomes. Sections were stained with aqueous cresyl violet acetate or double-stained with safranin and astra blue and observed with bright-field and polarized light to differentiate the developing xylem cells.

In total, data were collected from 814 individuals of 20 conifers distributed across 75 sites that covered boreal, temperate, Mediterranean, and subtropical biomes in North America, Europe, and Asia. The sites were distributed over latitudes from 23°11′ N to 66°12′ N and at elevations ranging from 23 m to 3850 m a.s.l. (Figure 3a and Table S1).

2.2 | Species classification

Early successional species are the shade-intolerant pioneers corresponding to life history strategies of fast growth rate and an ability

to grow in harsh conditions, whereas late successional species are those that are shade tolerant and characterized by a slow growth rate. There were 645 individuals belonging to the early successional species, that is, *Juniperus przewalskii* (JUPR), *Juniperus thurifera* (JUTH), *Larix decidua* (LADE), *Pinus halepensis* (PIHA), *Pinus heldreichii* (PIHE), *Pinus leucodermis* (PILE), *Pinus longaeva* (PILO), *Pinus massoniana* (PIMA), *Pinus peuce* (PIPE), *Pinus pinaster* (PIPI), *Pinus sylvestris* (PISY), *Pinus tabulaeformis* (PITA), *Pinus uncina* (PIUN). There were 1302 individuals belonging to the late successional species, that is, *Abies alba* (ABAL), *Abies balsamea* (ABBA), *Abies georgei* (ABGE), *Cedrus libani* (CELI), *Picea abies* (PCAB), *Picea mariana* (PCMA), and *Pinus cembra* (PICE). In general, the two successional species overlap along the MAT gradients, except the individuals of the early successional species located at warmer sites (Figure 1b). Three species, JUPR, JUTH, and PIHE, are unique species that grow in harsh conditions, show a slow growth rate and a long-life history. They cannot be grouped into early or late successional species according to classical theory; therefore, they were excluded when splitting the data into different successional stages and associated downstream analyses.

2.3 | Xylem phenology data

A common protocol for classifying xylem cells at different developmental phases was followed at all sites. For each sample, the number of cells in the cambial zone, and cells in the enlargement and secondary cell wall thickening phases were counted along three radial rows. Thin-walled enlarging cells were distinguished from cambial cells by their larger size, as they had a radial diameter at least twice that of a fusiform cambial cell (Deslauriers et al., 2003). A wall-thickening cell was differentiated from an enlarging cell by the presence of a secondary cell wall that displayed birefringence under polarized light due to the orientation of the cellulose microfibrils (Abe et al., 1997).

Color changes from violet to blue (simple cresyl violet acetate staining) or from blue to red (double safranin-astra blue staining) demonstrated the entire progression of wall thickening (Figure S2). Mature cells presented entirely lignified, monochromatic walls; therefore, the absence of cytoplasm and a complete color change over the whole cell wall marked the end of lignification and the full maturation of the tracheid (Abe et al., 1997). The mean number of xylem cells in the wall-thickening phase was obtained at each sampling date. The timing of the onset of wall thickening, represented by the day of the year (DOY), was defined for each tree, site, and year as the date of appearance of the first wall-thickening cell and was referred to as the cell-wall-thickening DOY.

2.4 | Statistical analyses

We explored key drivers of cell-wall-thickening DOY among six selected common potential predictors (MAT, photoperiod, forcing,

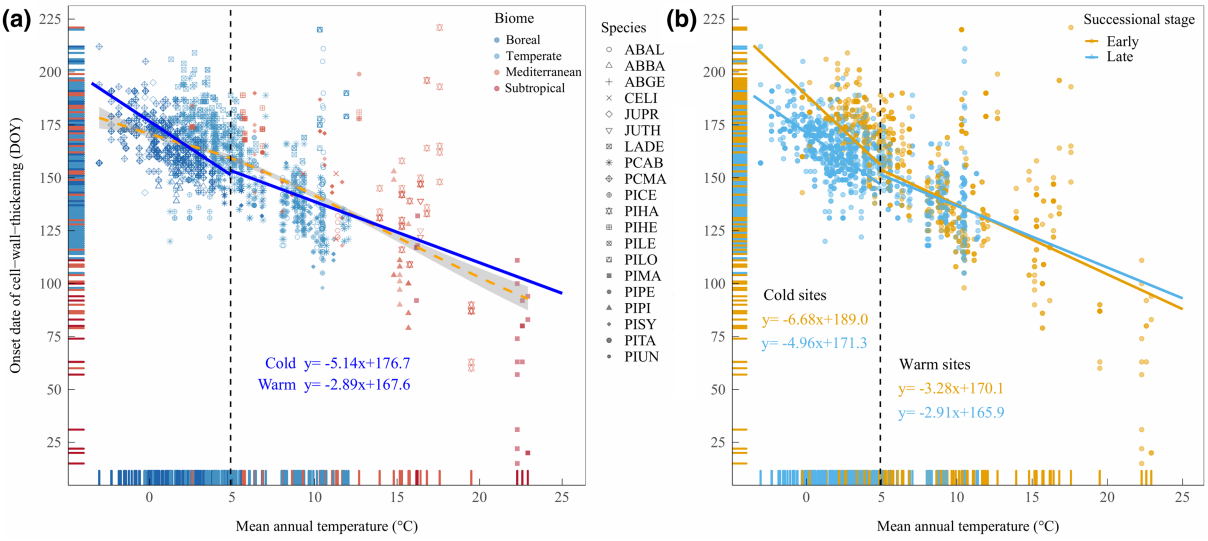

FIGURE 1 Changes in the cell-wall-thickening DOY (day of the year) separate along the mean annual temperature (MAT) gradients of the study sites, with contrasting slopes between cold and warm sites. According to the determined break point (at 4.9 ± 1.1°C), segmented regression lines (the solid lines) were fitted with linear mixed-effect models separately for all observations (a) and for early successional species and late successional species (b) at different temperature zones. The dashed orange line (a) was fitted with a generalized linear model for all observations. Species are reported with the following acronyms and classified into early (JUPR, *Juniperus przewalskii*; JUTH, *Juniperus thurifera*; LADE, *Larix decidua*; PIHA, *Pinus halepensis*; PIHE, *Pinus heldreichii*; PILE, *Pinus leucodermis*; PILO, *Pinus longaeva*; PIMA, *Pinus massoniana*; PIPE, *Pinus peuce*; PIPI, *Pinus pinaster*; PISY, *Pinus sylvestris*; PITA, *Pinus tabulaeformis*; and PIUN, *Pinus uncina*) and late (ABAL, *Abies alba*; ABBA, *Abies balsamea*; ABGE, *Abies georgei*; CELI, *Cedrus libani*; PCAB, *Picea abies*; PCMA, *Picea mariana*; PICE, *Pinus cembra*) successional species types (see Supporting information for further details). Points (n = 1948) represent individual trees from the 75 study sites included in this study. Biomes include boreal (b), temperate (T), Mediterranean (M), and subtropical (S). [Colour figure can be viewed at wileyonlinelibrary.com]

chilling, scPDSI, and spring temperature variation) using three classes of statistical models: boosted regression trees (BRTs), linear mixed-effect models (LMMs), and Bayesian mixed-effect models (BMMs). We also performed a natural cubic spline to check for the general trends among different predictor variables or between the cell-wall-thickening DOY and a certain selected predictor.

2.4.1 | General patterns: Settings and diagnostics for boosted regression trees

We assessed the relative importance of explanatory variables in predicting the cell-wall-thickening DOY using BRTs (Figure S3a), as these have been used extensively in ecological studies with an ensemble of 'boosted' multiple decision trees for analysis of complex systems (Frey et al., 2016; McClanahan et al., 2019). The fitting procedures for a BRT model do not make assumptions on data distribution for a large data set, and they have several advantages, such as collinearity handling among predictors and robustness to outliers (Elith et al., 2008), especially when accounting for nonlinear relationships and complex interactions between explanatory variables of multiple classes during boosted regression modeling (Venter et al., 2018). We used the following settings for our BRT model: a tree complexity of 10, a learning rate of 0.005, and a bag fraction of 0.7. A smaller learning rate corresponds to a higher number of trees used in the model, while the bag fraction was added as a stochastic component that improves model performance by reducing variance in the final model. A final BRT model with 5800 trees was chosen for our study.

A partial dependence plot following BRT modeling was then constructed to show the general trending pattern of the relationship between the cell-wall-thickening DOY and each predictor (Figure S3b–g). The R program packages "gbm" package, "dismo," and "pdp" were used for the BRT analyses and visualization (Muggeo, 2008).

After using the fitted BRT model to confirm MAT as the most important predictor (Figure S3a), we fitted a natural cubic spline (Ortiz-Bobea et al., 2018) to provide a nonlinear smoothed estimate of the other five predictors and frost frequency along the MAT gradient (Figure S4). Cubic spline regressions make no assumptions about the shape of a curve other than smoothness, and they are commonly suggested for examination of the fitness and performance of natural selection on a quantitative trait, such as the thermal performance traits (Logan et al., 2014). Cubic splines were estimated using the "mgcv" package.

2.4.2 | Breakpoint analysis: Cell-wall-thickening day of the year versus mean annual temperature

The preliminary analyses described above revealed an apparent transition of the relationship between cell-wall-thickening DOY and MAT from the BRT-related partial dependence plot (Figure S3b), indicating the possible existence of a thermal transition along the MAT gradient. We conducted a methodology for threshold detection following Berdugo et al. (2020). Specifically, we constructed generalized linear and segmented regressions to the relationships between cell-wall-thickening DOY and MAT with a log-linked Gaussian error distribution for the full data set using the R package "MASS" and the 'Segmented' R package (Muggeo, 2008) (Figure 1), respectively. We used AIC to decide the model that provided the best fit in each case (Hastie, 2017). This criterion lower than 2 indicates that the model is significantly better (Berdugo et al., 2020). Only when nonlinear regressions were a better fit to the data, thresholds may be present. Therefore, we explored the presence of thresholds only when nonlinear models were a better fit for the data. We fitted segmented regressions describing the point in the predictor (MAT) that evidences the shift in the relationship (in slope, intercept, or slope + intercept) between cell-wall-thickening DOY and MAT. We consider a threshold as the point in MAT in which the cell-wall-thickening DOY changes abruptly its value.

Next, to confirm the significance of the cell-wall-thickening trends (for overall observations and species referring to each successional stage) before and after the identified breakpoint (estimated at 4.9 ± 1.1°C), the full data set was split into cold (≤4.9°C) and warm (>4.9°C) temperature zones. Data in each temperature zone were obtained by further splitting into different sub-datasets according to their successional stages, that is, as early and late successional species.

Among the fitted segmented linear models, the statistical significance of the differences between the slopes of regressions was tested with standardized major axis (SMA) estimation (e.g., the difference in the regression slopes between temperature zones or successional stages) as implemented in the "smart" R package (Fox & Weisberg, 2018). We also chose robust SMA estimation, which handles outliers with Huber's M-estimator, because our SMA approaches are highly sensitive to outliers (Warton et al., 2012). All analyses were performed in R v.4.0.2.

2.4.3 | Linear mixed-effect model and Bayesian mixed-effect model settings and diagnostics

We further examined the direction and magnitude of the relationships between environmental predictors and site covariates with cell-wall-thickening DOY by fitting a LMM and BMM for both the overall data set and the sub-datasets. Summary statistics (raw mean, median, and quantiles) of all data sets were obtained (Table S2) by fitting intercept-only LMMs without fixed predictor variables, using "site" and "species" as random intercept terms.

The LMMs were used to test for the main effects of the explanatory variables on cell-wall-thickening DOY. We obtained the best model for each data set by performing model selection procedures to determine the best random-effects structure and the optimized fixed-effect structure through a backward stepwise model simplification, using all the explanatory variables in the fixed component for the most complex models (Table S3). Collinearity among variables

was detected by the variance inflation factor (vif), and the variables with vif <3 were retained. The most complex model was fitted using the following formula:

$$D_{ijk} = \alpha + \beta_1 \mathrm{MAT}_{ijk} + \beta_2 P_{ijk} + \beta_3 F_{ijk} + \beta_4 C_{ijk} + \beta_5 \mathrm{PDSI}_{ijk} + \beta_6 \mathrm{Tem\_variation}_{ijk} + a_i + b_j + \varepsilon,$$

where D_{ijk} is the date of onset of the first cell wall thickening of species i at site j in year k; MAT_{ijk}, P_{ijk}, F_{ijk}, $C_{ijk,}$ PDSI_{ijk}, and $\mathrm{Tem\_variation}_{ijk}$ are fixed effects and represent the MAT, photoperiod, forcing, chilling, scPDSI, and spring temperature variation corresponding to D_{ijk}, respectively; α is the intercept; β_1, β_2, $\beta_{3,}$ β_4, β_5, and β_6 are the slopes; a_i and b_j are the random effects of the site i and species j, respectively; and ε is the error term.

Log-likelihood ratio tests and F tests were used to perform backward elimination of non-significant random and fixed effects (Kuznetsova et al., 2014) (Table S3). In particular, the fixed effects were retained or removed based on changes in the AIC, with ΔAIC values of <−2 as a criterion to drop variables and on a likelihood ratio test with a p value (based on Satterthwaite approximation) higher than 0.05, through which a rigorous estimate of the most parsimonious model was retained. The validity of the assumptions of normality and homoscedasticity was examined using residual plots (Burnham et al., 2011). For each optimal LMM, the contributions of the fixed- and random-effects variables in explaining variation in the dependent variable (i.e., cell-wall-thickening DOY) were calculated by a variance-partitioning analysis to partition the variances attributable to each variable into the best-fitting model (Hoffman & Schadt, 2016). We reported the coefficients of the optimal model estimated by the restricted maximum likelihood approach, the bootstrap confidence interval (90% and 95%) calculated based on 1000 simulations, and the marginal and conditional R^2 values, which account for fixed and fixed plus random effects. All the statistical analyses associated with LMMs were conducted using the R packages "lme4," "MuMIn," and "lmerTest."

The magnitude and significance of the six predictors in determining cell-wall-thickening DOY were further examined by BMMs. We standardized and centered the numerical independent variables before analyses, thereby facilitating the direct comparison of the resulting coefficients. All explanatory variables were considered in these models, which we ran as four chains with 2000 iterations each, burning 1000 samples per chain, with analysis of 1000 post-warmup samples. Statistical significance was obtained by means of the posterior distribution of the 95% credible interval of its mean estimate (log odds ratio). Positive and negative values of the log odds ratio denote positive versus negative effects, respectively, while a significant effect occurs when no overlap exists between the 95% error bars and zero. The mean estimates (representing Bayesian probabilities) of BMMs were overall similar to the predictor ranking of variance-partitioning analysis obtained by LMMs, with minor differences for sub-dataset modelings partly due to different model structures and statistical approaches.

Finally, according to the identified temperature threshold (4.9°C) of tree xylem phenology under rising MAT, we mapped those regions vulnerable to such a critical transition in future climate warming scenarios (Figure 3b). These areas are selected by comparing the differences between two periods of MAT in the Northern Hemisphere (Figure S1), that is, recent MAT (1970–2000, from worldclim.org) versus future MAT (2061–2080, projected by CMIP5). We mapped those areas with MAT <4.9°C in recent temperature scenarios and future MAT exceeding the threshold value 4.9°C experiencing temperature rise, and considered that the spring phenology of coniferous trees in these regions is more vulnerable to the thermal transition identified and discussed in this study.

3 | RESULTS

3.1 | Thermal transition across temperature (MAT) gradient

We identified MAT as the major driver of cell-wall-thickening DOY among selected predictors with BRT analyses (Figure S3a). Partial dependence plot from BRT further showed that cell-wall-thickening DOY was a decreasing function of the rising MAT gradient (i.e., phenological advance) and responded in a nonlinear manner, with apparent thermal transitions along the descending trend (Figure S3b). A generalized segmented regression model assuming one breakpoint (AIC = 17,274.2 and BIC = 17,302.2) outperformed a generalized linear regression (AIC = 17,326.0 and BIC = 17,342.8) and supported such a hypothesized thermal transition. Observed temperature-scaling of the cell-wall-thickening DOY based on the piecewise model indicates a qualitative transition at MAT = 4.9 ± 1.1°C (Figure 1a). The slopes of the segments to the left (−5.14) and the right (−2.89) of the observed breakpoint differed significantly (Davies' test, p = .001). Consequently, this thermal transition separated our study sites into the cold and the warm ecosystems, whereby a significantly greater phenological advancement occurred in sites with MAT below 4.9 °C but a smaller advancement occurred in sites with MAT above 4.9°C, respectively (Figure 1a,b).

Accordingly, species with sufficient coverage along the MAT gradient, for example, *Picea abies* (n = 447, Figure S5), exhibited a significantly greater advancement in cold regions and a smaller advancement in warm areas (Figure S5; p = .001). At the biome level, both boreal and cold-temperate forests (MAT <4.9°C) showed a significantly stronger advancement than did the Mediterranean and warm-temperate forests (MAT >4.9°C) (Figure S7; p = .001). Previous studies have reported that early successional species are more responsive to rising temperature than are the late-successional ones (Basler & Körner, 2012; Fu et al., 2019), and therefore, we also considered them separately in the current study (see Species classification in Section 2 for further details). The early and late successional species also revealed similar patterns, that is, have smaller advancement when MAT >4.9°C (Figure 1b).

3.2 | The partition of variance of the main drivers

By constructing LMMs and BMMs, we explored the reasons underlying the decreased advancement to rising temperature and

assessed and quantified the main environmental drivers for the onset of cell-wall-thickening in cold versus warm ecosystems (see LMM and BMM settings and diagnostics in Statistical analyses for further details). The onset of the spring phenology of forest trees is also strongly regulated by local spring temperature variance and soil moisture availability (Huang et al., 2020; Körner & Basler, 2010), and these parameters were included in the LMMs and BMMs.

In the cold sites, MAT remained the main driver for the cell-wall-thickening DOY, while its relative importance substantially decreased in warm sites, where forcing superseded MAT as the major driver (Figure 2a,b,g). In determining the cell-wall-thickening DOY, photoperiod was more important in warm sites than in cold sites (Figure 2a,b,g). Similarly, chilling consistently explained higher variances of cell-wall-thickening DOY in warm sites than that in cold sites (Figure 2a,b,g).

In addition, the relative importance of selected phenological predictors differed between different successional stages, that is, early- versus late-successional species. MAT in regulating cell-wall-thickening DOY explained a higher variance for both early and late species in cold sites than in warm sites, especially for the early ones. Similarly, photoperiod was more important for the early species than the late species in warm sites (Figure 2c–g). Higher scPDSI delayed the cell-wall-thickening DOY, again more pronounced for the early species (Figure 2c–g).

At the biome level, MAT played a much more important role in determining cell-wall-thickening DOY in the boreal and cold-temperate forests than in the Mediterranean and warm-temperate forests (Figure S8). By contrast, forcing was the dominant driver for the Mediterranean and warm-temperate forests (Figure S8).

4 | DISCUSSION

Climate warming has resulted in more uniform spring phenology between cold (high latitudes or altitudes) and warm (low latitudes or altitudes) ecosystems (Chen et al., 2018; Chen et al., 2019; Ma et al., 2018; Meng et al., 2020), suggesting a possible existence of a thermal threshold across ecosystems over a large spatial scale. Such a threshold may separate the biomes into regions with diverging advancing rates of tree spring phenology under global warming, that is, a larger advancement at the higher latitudes or altitudes due to benefits from warming versus a smaller advancement at the lower latitudes or altitudes due to a higher forcing requirement induced by the reduced chilling accumulation. Our dataset showed evidence of an abrupt change in the advancement of cell wall thickening of conifers along the gradient in MAT over the Northern Hemisphere, corresponding with a threshold of 4.9 ± 1.1°C in MAT (Figure 1a,b).

The air temperature, represented by MAT in our analyses, was the primary factor regulating the timings of cell wall thickening in cold ecosystems, whereas forcing was the main trigger in warm ecosystems. Our results suggest that global warming would continue to advance the onset of cell wall thickening, but this advancement could slow down because of the increased requirement in forcing temperature in warm ecosystems. Our results provide empirical evidence for introducing a thermal transition into temperature-based models for a better understanding of thermal adaption mechanisms in their geographical context. This inclusion will improve Earth-System-Models for predicting global forest phenology, productivity and biogeochemical cycles under climate warming.

4.1 | A critical thermal transition revealed in the Northern Hemisphere

The abrupt change in the slopes of the advancement of cell-wall-thickening DOY (at MAT of 4.9 ± 1.1°C) (Figure 1a) has important ecological implications, implying divergent advancing rates of forest phenology events could be quantitatively organized into a larger-smaller advancement spectrum: larger advancements in cold sites and smaller advancements in warm sites. The advancement of cell-wall-thickening DOY to rising temperatures would significantly slow down at a MAT of 4.9°C. Our research extends and advances prior research reporting that the effects of climate warming on forest spring phenology are dependent on weather conditions (Gunderson et al., 2012; Montgomery et al., 2020). The greater advancement to rising temperature in cold ecosystems, associated with the reduction in advancement in warm ecosystems, could reduce spatial variability. Therefore, we would expect a more uniform trend in spring phenology between cold and warm ecosystems under ongoing warming conditions (Chen et al., 2019; Ettinger et al., 2020; Ma et al., 2018).

At the species level, as early successional species showed a stronger advancing shift in cold sites than that for the late-successional ones, these two functional groups would shift further apart under rising temperatures. Hence, the cold sites would face fundamental changes in the timing of cell wall thickening and the synchrony among tree species, with consequences for the plant communities and the whole ecosystem (Kharouba et al., 2018). However, the two successional groups showed a marginally similar degree of shift in warm sites (Figure 1b). Consequently, the early species exhibited a more substantial and abrupt decline in further advancement along the MAT gradient than did the late ones (Figure 1b).

4.2 | Drivers for cell wall thickening across the thermal threshold and underlying mechanisms

We explored key drivers of cell-wall-thickening DOY among six selected common potential predictors (MAT, photoperiod, forcing, chilling, scPDSI, and spring temperature variation, see climate data and photoperiod in Supplementary Information Text for further details) using LMMs and BMMs. The main environmental drivers varied greatly for trees in the cold versus warm temperature regimes. MAT

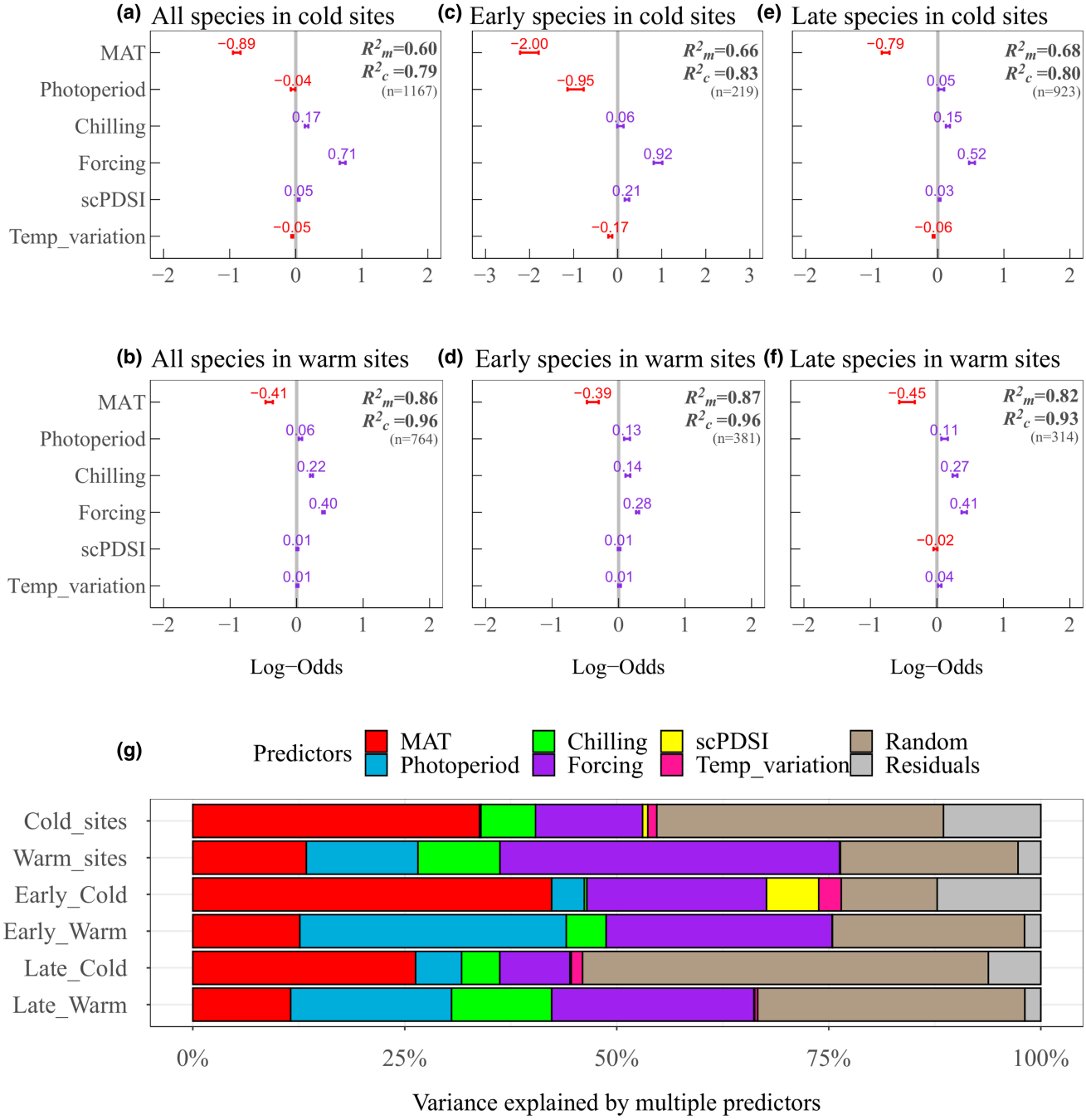

FIGURE 2 Summary of the direction and magnitude of the effect of all predictors on cell-wall-thickening day of the year (DOY) in different systems using Bayesian linear mixed-effect models, shown in (a–f), and including samples from different temperature zones: The upper (a, c, e) and lower (b, d, f) panels were from cold and warm sites, respectively. Samples were also assigned to different successional stages: Early species (c, d) and late species (e, f). Significant effects occur when no overlaps exist between the 95% error bars and zero. The blue and red colors denote positive versus negative effects, respectively. The Bayes factors are provided to show significance. Marginal and conditional *R*-squared (R^2_m and R^2_c, respectively) values are provided. Based on the best-fitting linear mixed-effect models (Table S3), variance partitioning of the selected fixed- and random-effects variables, indicating the relative importance of each predictor, is also shown in figure g, and the sample sizes are reported for each model. The variance inflation factor (vif) of each predictor variable in the linear mixed models is provided for all observations and subset modelings in Table S4. MAT: The mean annual temperature at each site per year; photoperiod: The length of time that an organism is exposed to sunlight each day, was calculated as the interval between sunrise and sunset for each site; chilling: The length of the period (days or hours) during which the temperature remains within the range of −5°C and 5°C, the reference period starting from November 1st of the previous year to the onset day of cell wall thickening; forcing: The length of period (days or hours) during which the temperature remains above 5°C, the reference period starting from January 1st to the onset day of cell wall thickening; scPDSI: The self-calibrating palmer drought severity index, representing soil moisture (scPDSI ranging from −4 to 4, indicating from excessively dry to excessively moist); Tem_variation: The averaged standard deviation of the mean daily temperature in a 60-day period over the mean cell-wall-thickening DOY (60-day centered period) at each site and in the same year, this value was used to represent the local spring temperature variance. [Colour figure can be viewed at wileyonlinelibrary.com]

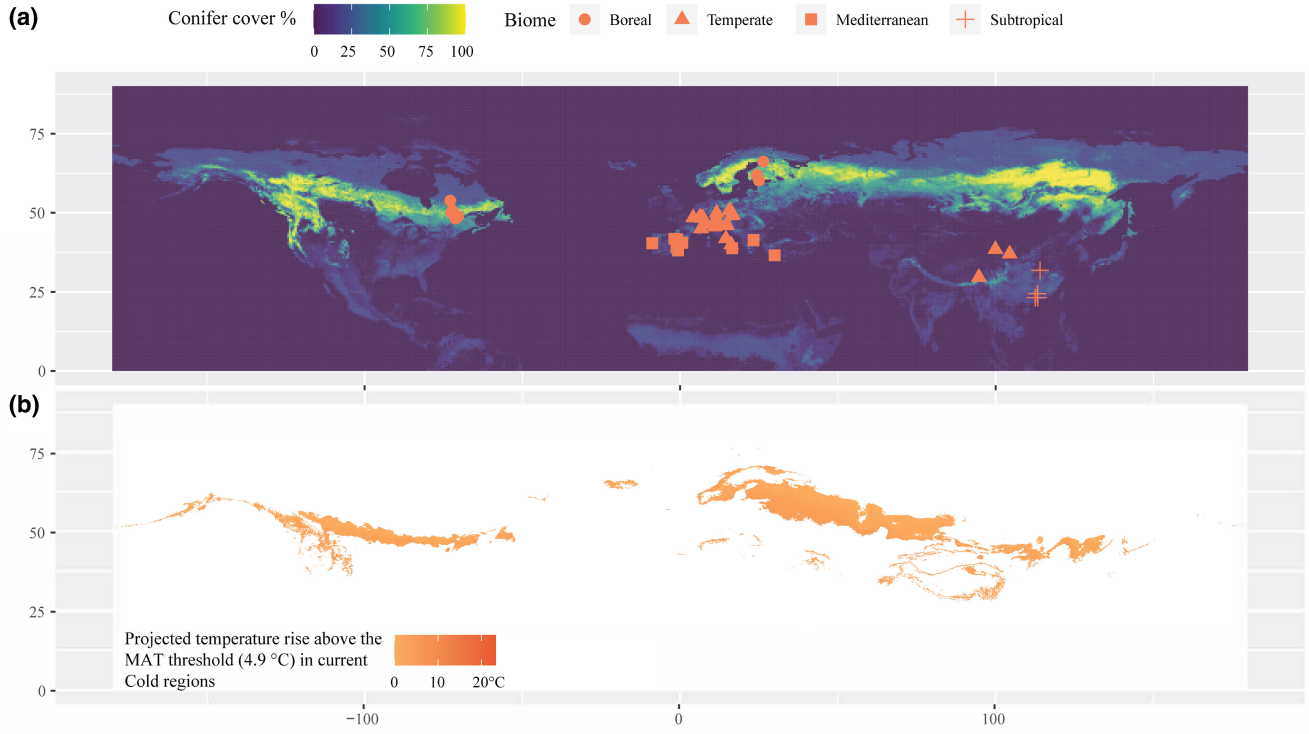

FIGURE 3 (a) Geographical distributions of global conifer cover (data from Global Forest Age Dataset (GFAD) (Poulter et al., 2019) and location of the study sites across the Northern Hemisphere. The numbers in the conifer cover legend denote the relative coniferous forest cover proportional to a specific total area in the GFAD (Poulter et al., 2019). (b) Areas in the current cold region (MAT <4.9°C) that may turn into warm regions in CMIP5 projected changes in MAT in the Northern Hemisphere. This is predicted by the differences in MAT between 1970 and 2000 (from worldclim.org) and between 2061 and 2080 (projected by CMIP5). [Colour figure can be viewed at wileyonlinelibrary.com]

was the reason behind most of the variance in the timings of cell wall thickening in cold ecosystems, but its relative importance dropped in warm ecosystems (Figure 2a,b,g). This confirmed that cell wall thickening in cold regions is strongly regulated by MAT. Therefore, the occurrence of the first xylem wall thickening cell becomes a matter of tracking the appropriate temperature across ecosystems and species (Begum et al., 2013; Rossi et al., 2016). Trees are subjected to selective pressure to match their spring phenology to favorable environmental conditions and minimize the risk of frost (Mura et al., 2022), while at the same time maximizing the length of the growing season to ensure trees safely complete secondary cell wall lignification before winter (Rossi et al., 2006). As the temperature is a limiting factor in cold and temperate climates, tracking global warming to obtain a long growing season and thus maximize annual carbon would become the priority of tree spring phenology.

In warmer ecosystems, the temperature rise would reduce the accumulation of chilling (Figure S4b), which could decrease the advancement of forest spring phenology to rising temperature (Chen et al., 2019; Ma et al., 2018; Meng et al., 2020). The greater variance in the timings of cell wall thickening explained by chilling in warm ecosystems demonstrates the possibility that the reduced chilling accumulation plays a role in reducing further advancement (Fu et al., 2015; Meng et al., 2020; Vitasse et al., 2018). However, the contribution of this factor was relatively small, suggesting that chilling was unable to explain completely the declining advancement of forest spring phenology, which is in line with previous studies (Ettinger et al., 2020; Fu et al., 2015). Instead, chilling exerted its influence mainly by improving the forcing requirement (Delpierre et al., 2019; Ma et al., 2018). Although increasing evidence ascribed the slowdown of the onset advancement of forest primary growth to a higher forcing temperature requirement induced by chilling insufficiency (Chen et al., 2019; Ma et al., 2018), it has only rarely been reported for the onset of xylem growth (Delpierre et al., 2019). Trees usually require exposure to a sufficient forcing temperature for the resumption of xylem cell growth (Delpierre et al., 2019). The higher accumulation of forcing temperatures in warm ecosystems (Figure S4c) was, thus, expected to advance the onset of cell wall thickening, but we observed declined advancing rate (Figure 1). We thus raise the hypothesis that a decreasing chilling exposure in warm sites (Figure S4b) induced a higher forcing requirement (Chen et al., 2019; Delpierre et al., 2019; Ma et al., 2018). Forcing is the most important factor in determining the timings of cell wall thickening in warm ecosystems (Figure 2), which supported our hypothesis. A photoperiod limitation for further advancement was also captured in our study, as indicated by the greater variance explained by the photoperiod in warm ecosystems compared with cold ecosystems (Figure 2) (Basler & Körner, 2012; Richardson et al., 2018; Zohner et al., 2016). The importance of the photoperiod was relatively low compared with forcing accumulation, in line with other studies showing that only a minor group (mainly from lower latitudes)

of temperate trees were constrained by day length (Rossi, 2015; Zohner et al., 2016). Our results illustrated how the environmental factors interact in space and result in the divergent advancing rates of forest spring phenology (Piao et al., 2019), thus providing a new perspective for understanding the potential trajectories of forest growth dynamics under global changes.

Notably, MAT had a dominant influence on early successional species in cold sites (Figure 2). This could be explained by the different life strategies, as they adopt more risky life strategies (Körner & Basler, 2010) and can better benefit from appropriate temperatures for cell wall thickening. By contrast, late successional species adopt more conservative strategies and are less responsive to rising temperatures, which reflects the process of natural selection in environments characterized by greater temperature fluctuations and higher frost frequency (Figure S9). There is evidence that early successional species are more likely to keep tracking climatic warming than late successional species (Basler & Körner, 2012; Fu et al., 2019; Körner & Basler, 2010). Moreover, once cross the transition, photoperiod and forcing temperatures had similar importance for early successional species.

To the best of our knowledge, this study is the first to provide a quantitative indication of the existence of a thermal threshold at MAT = 4.9 ± 1.1°C, based on a unique dataset describing the onset of cell wall thickening in Northern Hemisphere conifers. This thermal threshold classified all the studied sites into cold and warm ecosystems, where air temperature (represented by MAT) and forcing, respectively, were the primary drivers for triggering the onset of cell wall thickening. Rising temperatures will continue to advance the onset dates, but this advancement would significantly decline upon crossing the thermal transition toward warm ecosystems. Rising MAT in many areas of the Northern Hemisphere (Balting et al., 2021) may have exceeded certain threshold temperatures in recent two decades, leading to the widely observed declining phenology advancement (Fu et al., 2015; Vitasse et al., 2018). For areas in the current cold regions (MAT <4.9°C) that may turn into warm regions predicted by climatic models (Figure 3b), we would expect to see declining sensitivity of xylem phenology to warming similar to other spring phenological phases (Fu et al., 2015), particularly for those conifer trees inhabit within these areas (Figure 3b). The early and late successional species would be expected to shift further apart in cold ecosystems due to different advancing rates to rising temperatures. Conversely, in warm ecosystems, future global warming would exert less influence on the phenological synchrony between the early and late successional species due to their similar advancing rates. Our results overall demonstrate how forest spring phenology will respond to rising temperatures in two distinct phases, lending insights into the mechanisms behind the divergent results regarding phenological responses (Piao et al., 2019). The identified thermal threshold can thus be integrated into the Earth-System-Models to enable more accurate and reasonable predictions of global carbon, water, and energy cycles under global warming (Montgomery et al., 2020; Wolkovich et al., 2012).

AUTHOR CONTRIBUTIONS

JH, YL, and YZ designed this study. YZ, MW, and XY analyzed the data. YZ and JH wrote the manuscript with assistance from SR, MW, and YL. All co-authors contributed to this work in various ways including conducting field experiments, laboratory work, preprocessing, and contribution of data, as well as by commenting on and improving the manuscript.

ACKNOWLEDGMENTS

This work was primarily funded by the Xinjiang Regional Collaborative Innovation Project (2022E01045), the National Natural Science Foundation of China (32271653, 32001138 and 32001118), and Zhejiang University (108000*1942222R1). Other funding agencies included the Austrian Science Fund (FWF P22280-B16; P25643-B16), Observatoire régional de recherche en forêt boréale, Consortium de Recherche sur la Forêt Boréale Commerciale, Fonds de Recherche sur la Nature et les Technologies du Québec, Forêt d'enseignement et de recherche Simoncouche, Natural Sciences and Engineering Research Council of Canada, Slovenian Research Agency ARRS (young researchers' program, programs P4-0015 and P4-0107, and project Z4-7318), MIUR-PRIN 2002 (2002075152) and 2005 (2005072877), Swiss National Science Foundation (Projects INTEGRAL-121859 and LOTFOR-150205), French National Research Agency (ANR) as part of the "Investissements d'Avenir" program (ANR-11-LABX-0002-01, Lab of Excellence ARBRE), Academy of Finland (Nos. 250299, 257641 and 265504), NSFC (41525001), Grant Agency of Czech Republic (P504/11/P557), and Provincia Autonoma di Trento (project "SOFIE 2"–3012/2007) and Russian Science Foundation (22-14-00048). The cooperation among authors was supported by the EU COST Action FP1106 STReESS. The views and conclusions contained in this document are those of the authors and should not be interpreted as representing the opinions or policies of the funding agencies and supporting institutions.

CONFLICT OF INTEREST

The authors declare that they have no competing interests.

DATA AVAILABILITY STATEMENT

The raw data supporting the findings of this study are openly available from the following URL: https://doi.org/10.5061/dryad.pc866t1sk. Other supporting climate data are openly available from National Oceanic and Atmospheric Administration (NOAA) at the following URL: https://www.ncdc.noaa.gov/cdo-web/datatools/findstation. The Global Forest Age Dataset is openly available from the following URL: https://doi.pangaea.de/10.1594/PANGAEA.889943.

ORCID

Yaling Zhang https://orcid.org/0000-0002-7363-3138
Patrick Fonti https://orcid.org/0000-0002-7070-3292
Eryuan Liang https://orcid.org/0000-0002-8003-4264
Václav Treml https://orcid.org/0000-0001-5067-3308
Bao Yang https://orcid.org/0000-0002-1063-351X

Jiao-Lin Zhang https://orcid.org/0000-0003-3693-7965
Jesus Julio Camarero https://orcid.org/0000-0003-2436-2922
Filipe Campelo https://orcid.org/0000-0001-6022-9948
Yu Liu https://orcid.org/0000-0002-1402-0737

REFERENCES

Abe, H., Funada, R., Ohtani, J., & Fukazawa, K. (1997). Changes in the arrangement of cellulose microfibrils associated with the cessation of cell expansion in tracheids. *Trees*, *11*(6), 328–332.

Antonucci, S., Rossi, S., Deslauriers, A., Lombardi, F., Marchetti, M., & Tognetti, R. (2015). Synchronisms and correlations of spring phenology between apical and lateral meristems in two boreal conifers. *Tree Physiology*, *35*(10), 1086–1094.

Asse, D., Chuine, I., Vitasse, Y., Yoccoz, N. G., Delpierre, N., Badeau, V., Delestrade, A., & Randin, C. F. (2018). Warmer winters reduce the advance of tree spring phenology induced by warmer springs in the Alps. *Agricultural and Forest Meteorology*, *252*, 220–230.

Balting, D. F., AghaKouchak, A., Lohmann, G., & Ionita, M. (2021). Northern hemisphere drought risk in a warming climate. *NPJ Climate and Atmospheric Science*, *4*, 61.

Basler, D., & Körner, C. (2012). Photoperiod sensitivity of bud burst in 14 temperate forest tree species. *Agricultural and Forest Meteorology*, *165*, 73–81.

Begum, S., Kudo, K., Rahman, M. H., Nakaba, S., Yamagishi, Y., Nabeshima, E., Nugroho, W. D., Oribe, Y., Kitin, P., & Jin, H.-O. (2018). Climate change and the regulation of wood formation in trees by temperature. *Trees*, *32*(1), 3–15.

Begum, S., Nakaba, S., Yamagishi, Y., Oribe, Y., & Funada, R. (2013). Regulation of cambial activity in relation to environmental conditions: Understanding the role of temperature in wood formation of trees. *Physiologia Plantarum*, *147*(1), 46–54.

Berdugo, M., Delgado-Baquerizo, M., Soliveres, S., Hernández-Clemente, R., Zhao, Y., Gaitán, J. J., Gross, N., Saiz, H., Maire, V., Lehmann, A., Rillig, M. C., Solé, R. V., & Lehmann, A. (2020). Global ecosystem thresholds driven by aridity. *Science*, *367*(6479), 787–790.

Burnham, K. P., Anderson, D. R., & Huyvaert, K. P. (2011). AIC model selection and multimodel inference in behavioral ecology: Some background, observations, and comparisons. *Behavioral Ecology and Sociobiology*, *65*(1), 23–35.

Chen, L., Huang, J. G., Ma, Q., Hänninen, H., Rossi, S., Piao, S., & Bergeron, Y. (2018). Spring phenology at different altitudes is becoming more uniform under global warming in Europe. *Global Change Biology*, *24*(9), 3969–3975.

Chen, L., Huang, J. G., Ma, Q., Hänninen, H., Tremblay, F., & Bergeron, Y. (2019). Long-term changes in the impacts of global warming on leaf phenology of four temperate tree species. *Global Change Biology*, *25*(3), 997–1004.

Cuny, H. E., Rathgeber, C. B., Frank, D., Fonti, P., Mäkinen, H., Prislan, P., Rossi, S., Del Castillo, E. M., Campelo, F., Vavrčík, H., Camarero, J. J., Bryukhanova, M. V., Jyske, T., Gričar, J., Gryc, V., De Luis, M., Vieira, J., Čufar, K., Kirdyanov, A. V., … Vavrčík, H. (2015). Woody biomass production lags stem-girth increase by over one month in coniferous forests. *Nature Plants*, *1*(11), 1–6.

Delpierre, N., Lireux, S., Hartig, F., Camarero, J. J., Cheaib, A., Čufar, K., Cuny, H., Deslauriers, A., Fonti, P., Gričar, J., Huang, J. G., Krause, C., Liu, G., de Luis, M., Mäkinen, H., Del Castillo, E. M., Morin, H., Nöjd, P., Oberhuber, W., … Gričar, J. (2019). Chilling and forcing temperatures interact to predict the onset of wood formation in northern hemisphere conifers. *Global Change Biology*, *25*(3), 1089–1105.

Delpierre, N., Vitasse, Y., Chuine, I., Guillemot, J., Bazot, S., & Rathgeber, C. B. (2016). Temperate and boreal forest tree phenology: From organ-scale processes to terrestrial ecosystem models. *Annals of Forest Science*, *73*(1), 5–25.

Deslauriers, A., Morin, H., & Begin, Y. (2003). Cellular phenology of annual ring formation of *Abies balsamea* in the Quebec boreal forest (Canada). *Canadian Journal of Forest Research*, *33*(2), 190–200.

Elith, J., Leathwick, J. R., & Hastie, T. (2008). A working guide to boosted regression trees. *Journal of Animal Ecology*, *77*(4), 802–813.

Elmendorf, S. C., Henry, G. H., Hollister, R. D., Fosaa, A. M., Gould, W. A., Hermanutz, L., Hofgaard, A., Jónsdóttir, I. S., Jorgenson, J. C., Lévesque, E., Magnusson, B., Molau, U., Myers-Smith, I. H., Oberbauer, S. F., Rixen, C., Tweedie, C. E., & Lévesque, E. (2015). Experiment, monitoring, and gradient methods used to infer climate change effects on plant communities yield consistent patterns. *Proceedings of the National Academy of Sciences of the United States of America*, *112*(2), 448–452.

Ettinger, A., Chamberlain, C., Morales-Castilla, I., Buonaiuto, D., Flynn, D., Savas, T., Samaha, J. A., & Wolkovich, E. (2020). Winter temperatures predominate in spring phenological responses to warming. *Nature Climate Change*, *10*(12), 1137–1142.

Fox, J., & Weisberg, S. (2018). *An R companion to applied regression*. Sage publications.

Frey, S. J., Hadley, A. S., Johnson, S. L., Schulze, M., Jones, J. A., & Betts, M. G. (2016). Spatial models reveal the microclimatic buffering capacity of old-growth forests. *Science Advances*, *2*(4), e1501392.

Fu, Y. H., Piao, S., Zhou, X., Geng, X., Hao, F., Vitasse, Y., & Janssens, I. A. (2019). Short photoperiod reduces the temperature sensitivity of leaf-out in saplings of *Fagus sylvatica* but not in horse chestnut. *Global Change Biology*, *25*(5), 1696–1703.

Fu, Y. H., Zhao, H., Piao, S., Peaucelle, M., Peng, S., Zhou, G., Ciais, P., Huang, M., Menzel, A., Peñuelas, J., Song, Y., Vitasse, Y., Zeng, Z., & Peñuelas, J. (2015). Declining global warming effects on the phenology of spring leaf unfolding. *Nature*, *526*(7571), 104–107.

Gunderson, C. A., Edwards, N. T., Walker, A. V., O'Hara, K. H., Campion, C. M., & Hanson, P. J. (2012). Forest phenology and a warmer climate–growing season extension in relation to climatic provenance. *Global Change Biology*, *18*(6), 2008–2025.

Hastie, T. J. (2017). Generalized additive models. In *Statistical models in S* (pp. 249–307). Routledge.

Hoffman, G. E., & Schadt, E. E. (2016). variancePartition: Interpreting drivers of variation in complex gene expression studies. *BMC Bioinformatics*, *17*(1), 1–13.

Huang, J.-G., Ma, Q., Rossi, S., Biondi, F., Deslauriers, A., Fonti, P., & Liang, E. (2020). Photoperiod and temperature as dominant environmental drivers triggering secondary growth resumption in northern hemisphere conifers. *Proceedings of the National Academy of Sciences of the United States of America*, *117*(34), 20645–20652.

Kharouba, H. M., Ehrlén, J., Gelman, A., Bolmgren, K., Allen, J. M., Travers, S. E., & Wolkovich, E. M. (2018). Global shifts in the phenological synchrony of species interactions over recent decades. *Proceedings of the National Academy of Sciences of the United States of America*, *115*(20), 5211–5216.

Körner, C., & Basler, D. (2010). Phenology under global warming. *Science*, *327*(5972), 1461–1462.

Kuznetsova, A., Brockhoff, P. B., & Christensen, R. H. B. (2014). *lmerTest*: Tests for random and fixed effects for linear mixed effect models. R package version 2.0–11. http://CRAN.R-project.org/package=lmerTest

Logan, M. L., Cox, R. M., & Calsbeek, R. (2014). Natural selection on thermal performance in a novel thermal environment. *Proceedings of the National Academy of Sciences of the United States of America*, *111*(39), 14165–14169.

Ma, Q., Huang, J.-G., Hänninen, H., & Berninger, F. (2018). Reduced geographical variability in spring phenology of temperate trees with recent warming. *Agricultural and Forest Meteorology*, *256*, 526–533.

McClanahan, T. R., Darling, E. S., Maina, J. M., Muthiga, N. A., D'agata, S., Jupiter, S. D., Arthur, R., Wilson, S. K., Mangubhai, S., Nand, Y., Ussi, A. M., Humphries, A. T., Patankar, V. J., Guillaume, M. M. M., Keith, S. A., Shedrawi, G., Julius, P., Grimsditch, G., Ndagala, J., & Nand, Y. (2019). Temperature patterns and mechanisms influencing coral bleaching during the 2016 El Niño. *Nature Climate Change*, *9*(11), 845–851.

Meng, L., Mao, J., Zhou, Y., Richardson, A. D., Lee, X., Thornton, P. E., Ricciuto, D. M., Li, X., Dai, Y., Shi, X., & Jia, G. (2020). Urban warming advances spring phenology but reduces the response of phenology to temperature in the conterminous United States. *Proceedings of the National Academy of Sciences of the United States of America*, *117*(8), 4228–4233.

Menzel, A., Sparks, T. H., Estrella, N., Koch, E., Aasa, A., Ahas, R., Ricciuto, D. M., Li, X., Dai, Y., Shi, X., & Briede, A. (2006). European phenological response to climate change matches the warming pattern. *Global Change Biology*, *12*(10), 1969–1976.

Montgomery, R. A., Rice, K. E., Stefanski, A., Rich, R. L., & Reich, P. B. (2020). Phenological responses of temperate and boreal trees to warming depend on ambient spring temperatures, leaf habit, and geographic range. *Proceedings of the National Academy of Sciences of the United States of America*, *117*(19), 10397–10405.

Moser, L., Fonti, P., Büntgen, U., Esper, J., Luterbacher, J., Franzen, J., & Frank, D. (2010). Timing and duration of European larch growing season along altitudinal gradients in the Swiss Alps. *Tree Physiology*, *30*(2), 225–233.

Muggeo, V. M. (2008). Segmented: An R package to fit regression models with broken-line relationships. *R News*, *8*(1), 20–25.

Mura, C., Buttò, V., Silvestro, R., Deslauriers, A., Charrier, G., Raymond, P., & Rossi, S. (2022). The early bud gets the cold: Diverging spring phenology drives exposure to late frost in a *Picea mariana* [(mill.) BSP] common garden. *Physiologia Plantarum*, *174*, e13798.

Oribe, Y., Funada, R., & Kubo, T. (2003). Relationships between cambial activity, cell differentiation and the localization of starch in storage tissues around the cambium in locally heated stems of *Abies sachalinensis* (Schmidt) masters. *Trees*, *17*(3), 185–192.

Ortiz-Bobea, A., Knippenberg, E., & Chambers, R. G. (2018). Growing climatic sensitivity of US agriculture linked to technological change and regional specialization. *Science Advances*, *4*(12), eaat4343.

Peters, M. K., Hemp, A., Appelhans, T., Becker, J. N., Behler, C., Classen, A., Detsch, F., Ensslin, A., Ferger, S. W., Frederiksen, S. B., Gebert, F., Gerschlauer, F., Gütlein, A., Helbig-Bonitz, M., Hemp, C., Kindeketa, W. J., Kühnel, A., Mayr, A. V., Mwangomo, E., … Frederiksen, S. B. (2019). Climate–land-use interactions shape tropical mountain biodiversity and ecosystem functions. *Nature*, *568*(7750), 88–92.

Piao, S., Liu, Q., Chen, A., Janssens, I. A., Fu, Y., Dai, J., Liu, L., Lian, X., Shen, M., & Zhu, X. (2019). Plant phenology and global climate change: Current progresses and challenges. *Global Change Biology*, *25*(6), 1922–1940.

Poulter, B., Aragão, L., Andela, N., Bellassen, V., Ciais, P., Kato, T., Xin, L., Baatarbileg, N., Sebastiaan, L., Niel, P., Philippe, P., Shilong, P., Sassan, S., Dmitry, S., Martjan, S., & Shivdenko, A. (2019). The global forest age dataset and its uncertainties (GFADv1. 1).

Prevéy, J., Vellend, M., Rüger, N., Hollister, R. D., Bjorkman, A. D., Myers-Smith, I. H., Elmendorf, S. C., Clark, K., Cooper, E. J., Elberling, B., Fosaa, A. M., Henry, G. H. R., Høye, T. T., Jónsdóttir, I. S., Klanderud, K., Lévesque, E., Mauritz, M., Molau, U., Natali, S. M., … Elberling, B. (2017). Greater temperature sensitivity of plant phenology at colder sites: Implications for convergence across northern latitudes. *Global Change Biology*, *23*(7), 2660–2671.

Richardson, A. D., Hufkens, K., Milliman, T., Aubrecht, D. M., Furze, M. E., Seyednasrollah, B., Krassovski, M. B., Latimer, J. M., Nettles, W. R., Hanson, P. J., Warren, J. M., & Heiderman, R. R. (2018). Ecosystem warming extends vegetation activity but heightens vulnerability to cold temperatures. *Nature*, *560*(7718), 368–371.

Richardson, A. D., Keenan, T. F., Migliavacca, M., Ryu, Y., Sonnentag, O., & Toomey, M. (2013). Climate change, phenology, and phenological control of vegetation feedbacks to the climate system. *Agricultural and Forest Meteorology*, *169*, 156–173.

Rossi, S. (2015). Local adaptations and climate change: Converging sensitivity of bud break in black spruce provenances. *International Journal of Biometeorology*, *59*(7), 827–835.

Rossi, S., Anfodillo, T., Čufar, K., Cuny, H. E., Deslauriers, A., Fonti, P., Frank, D., Gričar, J., Gruber, A., Huang, J. G., Jyske, T., Kašpar, J., King, G., Krause, C., Liang, E., Mäkinen, H., Morin, H., Nöjd, P., Oberhuber, W., … Huang, J. G. (2016). Pattern of xylem phenology in conifers of cold ecosystems at the northern hemisphere. *Global Change Biology*, *22*(11), 3804–3813.

Rossi, S., Deslauriers, A., Anfodillo, T., Morin, H., Saracino, A., Motta, R., & Borghetti, M. (2006). Conifers in cold environments synchronize maximum growth rate of tree-ring formation with day length. *New Phytologist*, *170*(2), 301–310.

Venter, Z., Cramer, M., & Hawkins, H.-J. (2018). Drivers of woody plant encroachment over Africa. *Nature Communications*, *9*(1), 1–7.

Vitasse, Y., Signarbieux, C., & Fu, Y. H. (2018). Global warming leads to more uniform spring phenology across elevations. *Proceedings of the National Academy of Sciences of the United States of America*, *115*(5), 1004–1008.

Warton, D. I., Duursma, R. A., Falster, D. S., & Taskinen, S. (2012). Smatr 3–an R package for estimation and inference about allometric lines. *Methods in Ecology and Evolution*, *3*(2), 257–259.

Wolkovich, E. M., Cook, B. I., Allen, J. M., Crimmins, T. M., Betancourt, J. L., Travers, S. E., Pau, S., Regetz, J., Davies, T. J., Kraft, N. J., Ault, T. R., Bolmgren, K., Mazer, S. J., McCabe, G. J., McGill, B. J., Parmesan, C., Salamin, N., Schwartz, M. D., & Cleland, E. E. (2012). Warming experiments underpredict plant phenological responses to climate change. *Nature*, *485*(7399), 494–497.

Zohner, C. M., Benito, B. M., Svenning, J.-C., & Renner, S. S. (2016). Day length unlikely to constrain climate-driven shifts in leaf-out times of northern woody plants. *Nature Climate Change*, *6*(12), 1120–1123.

SUPPORTING INFORMATION

Additional supporting information can be found online in the Supporting Information section at the end of this article.

How to cite this article: Huang, J.-G., Zhang, Y., Wang, M., Yu, X., Deslauriers, A., Fonti, P., Liang, E., Mäkinen, H., Oberhuber, W., Rathgeber, C. B. K., Tognetti, R., Treml, V., Yang, B., Zhai, L., Zhang, J.-L., Antonucci, S., Bergeron, Y., Camarero, J. J., Campelo, F. … Rossi, S. (2023). A critical thermal transition driving spring phenology of Northern Hemisphere conifers. *Global Change Biology*, *29*, 1606–1617. https://doi.org/10.1111/gcb.16543